Diffraction-limited two-dimensional hard-x-ray focusing at the 100 nm level using a Kirkpatrick-Baez mirror arrangement

S. Matsuyama, H. Mimura, and H. Yumoto
Department of Precision Science and Technology, Graduate School of Engineering, Osaka University, 2-1 Yamada-oka, Suita, Osaka 565-0871, Japan

K. Yamamura
Research Center for Ultra-Precision Science and Technology, Graduate School of Engineering, Osaka University, 2-1 Yamada-oka, Suita, Osaka 565-0871, Japan

Y. Sano
Department of Precision Science and Technology, Graduate School of Engineering, Osaka University, 2-1 Yamada-oka, Suita, Osaka 565-0871, Japan

K. Endo and Y. Mori
Research Center for Ultra-Precision Science and Technology, Graduate School of Engineering, Osaka University, 2-1 Yamada-oka, Suita, Osaka 565-0871, Japan

Y. Nishino, K. Tamasaku, and T. Ishikawa
SPring-8/RIKEN, 1-1-1 Kouto, Mikazuki, Hyogo 679-5148, Japan

M. Yabashi
SPring-8/Japan Synchrotron Radiation Research Institute (JASRI), 1-1-1 Kouto, Mikazuki, Hyogo 679-5148, Japan

K. Yamauchi
Department of Precision Science and Technology, Graduate School of Engineering, Osaka University, 2-1 Yamada-oka, Suita, Osaka 565-0871, Japan

(Received 28 January 2005; accepted 22 June 2005; published online 4 August 2005)

The spatial resolution of scanning x-ray microscopy depends on the beam size of focused x rays. Recently, nearly diffraction-limited line focusing has been achieved using elliptical mirror optics at the 100 nm level. To realize such focusing two-dimensionally in a Kirkpatrick-Baez system, the required accuracies of the mirror aligners in this system were estimated using optical simulators based on geometrical or wave-optical theories. A focusing unit fulfilling the required adjustment accuracies was constructed. The relationships between alignment errors and focused beam profiles were quantitatively examined at the 1 km long beamline (BL29XUL) of SPring-8 to be in good agreement with the simulation results. © *2005 American Institute of Physics.*
[DOI: 10.1063/1.2005427]

I. INTRODUCTION

In third-generation synchrotron radiation facilities such as SPring-8, ESRF, and APS, bright and coherent x-ray beams with low emittances are available. To utilize an x-ray beam preserving such excellent properties, x-ray optical devices having an unprecedently high degree of accuracy are required. For focusing x-ray beams, an x-ray mirror is a good device due to achromatic and efficient focusing. Recently, focusing performance using x-ray mirrors has improved significantly.[1–4]

In total-reflection mirror systems for hard x rays, ray-trace methods based on geometrical optics are mainly used to evaluate steered beam properties.[5] However, in such methods, the wavelength is assumed to be infinitely small so that focused beam profiles at nearly diffraction-limited operation cannot be evaluated. Recently, such focusing has been realized in hard x rays by mirror optics,[1,2] and new simulation methods based on wave optics[6] are highly demanded to evaluate the details of the beam performances.

In this study, a simulation code was developed, by which the necessary accuracy in a mirror alignment in a K-B-type[7] hard-x-ray focusing unit is estimated. The simulator was based on two theories of geometrical and wave optics according to the required accuracy. Geometrical optics was mainly employed in the estimation of the necessary accuracies in the alignments of the in-plane rotation, which is defined as the rotation around the normal of the surface at the center of the mirror, and the perpendicularity between the normals of two mirrors. Wave optics was utilized to estimate the required accuracy in the glancing angle adjustment. The calculated results showed that the glancing angle adjuster requires a microradian-level resolution. The accuracies in other alignments are indicated to be not significantly high; thus, to fulfill such a requirement is not so difficult. A focusing unit having the required alignment resolutions was actually developed and set at the 1 km long beamline (BL29XUL)[8] of SPring-8, and the relationships between the alignment errors and focused beam profiles were investi-

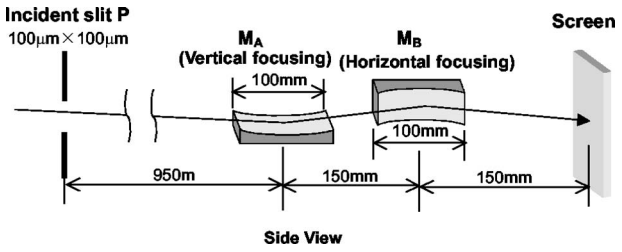

FIG. 1. Configuration of the optical system. The employed system is fitted to BL29XUL of Spring-8.

gated. The obtained results were in good agreement with the calculated results. Beam waist structures were also examined to understand the field depth as a probe in scanning x-ray microscopy.

II. OPTICAL CONFIGURATIONS

The optical configuration of a K-B-type focusing system in this study is shown in Fig. 1. The optical parameters are shown in Table I. The mirror M_A placed upstream is an elliptical mirror having a longitudinal length of 100 mm and a focal length of 300 mm for vertical focusing. The mirror M_B placed downstream is also an elliptical mirror having the same longitudinal length and a focal length of 150 mm for horizontal focusing. The distance between the centers of M_A and M_B is 150 mm. The principal dimensions employed are those of BL29XUL. The incident aperture of 100 μm $\times$100 μm is located 950 m upstream from the center of M_A. The work distance in this case is 100 mm, which is sufficient for various applications such as scanning x-ray microscopy or projection microscopy. The surface material of the mirrors is single crystal silicon. Figures of the mirror surface are designed to be effective for x rays with a photon energy smaller than 20 keV.

III. ALIGNMENT ACCURACIES OF PERPENDICULARITY OF TWO MIRRORS AND IN-PLANE ROTATIONS

The relationship between the adjustment error in the perpendicularity of two mirrors and the beam size broadening was investigated using the simulator based on geometrical optics. The arrival points of x rays on the screen under ideal alignment conditions are shown in Fig. 2. The influence of alignment error in the perpendicularity on beam size is shown in Fig. 3(a). Beam size is defined as the full width in the horizontal or vertical direction. The dotted lines indicate

TABLE I. Parameters of the elliptical mirrors.

	M_A mirror	M_B mirror
Glancing angle[a]	1.40 mrad	1.48 mrad
Focal length	300 mm	150 mm
Mirror length	100 mm	100 mm
Mirror width	5 mm	5 mm
Length of ellipse	1000.30 m	1000.30 m
Breadth of ellipse	48.50 mm	36.18 mm
Incident slit size	100 μm	100 μm

[a]Glancing angles are defined at the centers of the mirrors.

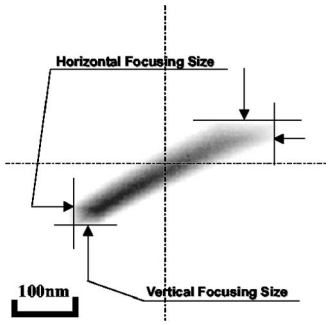

FIG. 2. Typical result of the arrival points of rays on the screen.

the predicted beam sizes in the diffraction-limited focusing of M_A and M_B. They are determined using the following equation, which is effective for the rectangular aperture:[9]

$$d = 2.0 \cdot \lambda \cdot f/D, \tag{1}$$

where d is the beam size defined as the distance between the first minimums, f is the focal length, λ is the wavelength of the x rays, and D is the aperture size of the relevant mirror, given by the product of the mirror length and the glancing angle. As understood from the intersecting points between the solid and dotted lines in Fig. 3(a), the acceptable range of the angle error is ±0.4 mrad for the realization of diffraction-limited focusing.

The relationship between the in-plane rotation error of each mirror and the beam is shown in Fig. 3(b). The horizontal and vertical axes denote the error angle and beam size, respectively. Beam size is defined as the maximum width also in this figure. The dotted lines in the graph indicate the predicted beam sizes in the diffraction-limited focusing. For the achievement of such focusing, the acceptable ranges of the angle errors in M_A and M_B are indicated to be ±65 mrad and ±40 mrad, respectively.

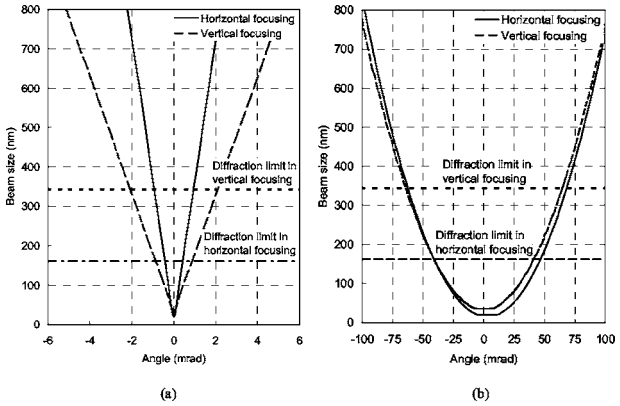

FIG. 3. Relationships between the beam size defined as the maximum width and mirror alignment errors of (a) the perpendicularity and (b) in-plane rotation of M_A and M_B. The dotted lines in the graph indicate the predicted beam sizes, which are defined as the distance between the first minimum points, in diffraction-limited focusing. (a) Perpendicularity of M_A and M_B. (b) In-plane rotation of M_A and M_B.

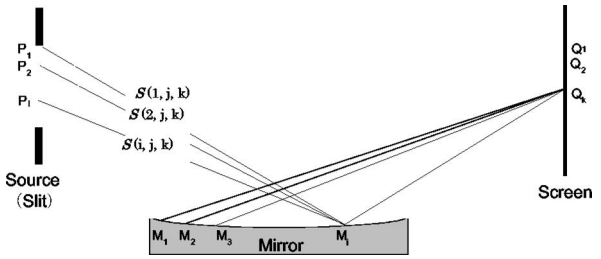

FIG. 4. Geometrical relationships among the x-ray source, mirrors, and screen in the simulator.

IV. GLANCING ANGLE ACCURACIES IN MIRROR ALIGNMENTS

A. Wave-optical simulation model

In the glancing angle alignment, a high accuracy is required; thus a wave-optical simulator is employed to estimate the accuracy criteria. In simulation using the ray-trace method, the full width of the focal image was employed as the beam size to avoid ambiguities of intensity distribution on the image plane. In this section, the beam sizes obtained by wave optics are discussed using full width at half maximum (FWHM) for the ease of comparison between the calculated and experimentally obtained beam sizes. The geometrical relationships among the x-ray source, mirrors, and screen in the simulator are set, as shown in Fig. 4. To determine the intensity distribution of the focused x rays, the Fresnel-Kirchhoff integrals[9] shown in Eq. (2) are calculated. In this code, the degree of coherence of the x-ray beam at the incident aperture can be taken into account:

$$I_Q(k) = \sum_{i=1}^{N_S}\sum_{j=1}^{N_M} |\alpha(i,j,k)|^2 I_S(i) + \sum_{i_1=1}^{N_S}\sum_{i_2>i_1}^{N_S}\sum_{j_1=1}^{N_M}\sum_{j_2>j_1}^{N_M} 2|\alpha(i_1,j_1,k)\alpha(i_2,j_2,k)|\mu(i_1,i_2) \times \exp\left\{\frac{2\pi i}{\lambda}(S(i_1,j_1,k) - S(i_2,j_2,k))\right\}. \quad (2)$$

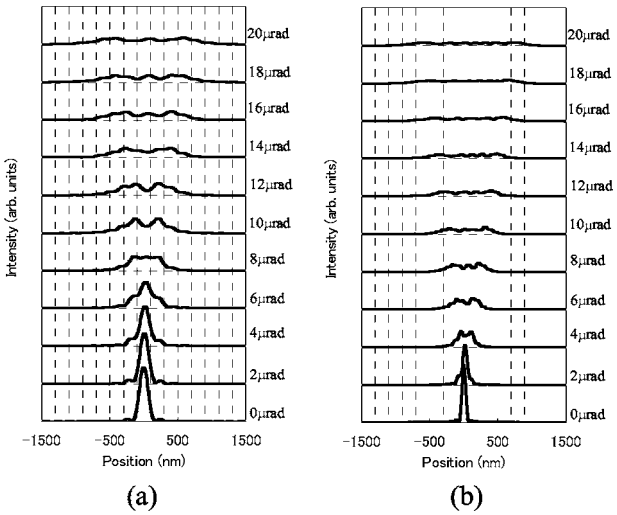

FIG. 5. Beam profiles at every 1 μrad error from the optimum angle in the x-ray energy of 15 keV. (a) Vertical focusing; (b) horizontal focusing.

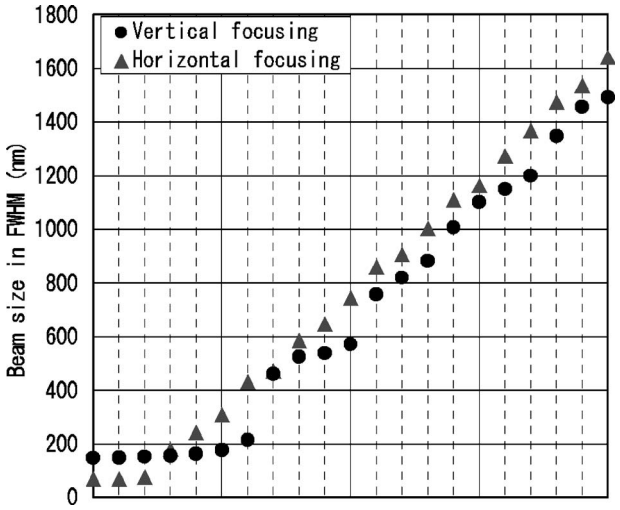

FIG. 6. Relationship between glancing angle errors and focusing beam profile, where the beam size was defined as FWHM.

Here, $I_Q(k)$ and $I_S(i)$ are the x-ray intensities at point k on the screen and at point i on the aperture, and $S(i,j,k)$ and $\alpha(i,j,k)$ are the distance and inclination factor from point i on the aperture to point k on the screen via point j on the mirror, respectively. $\mu(i_1,i_2)$ is the degree of coherency between points i_1 and i_2 on the aperture. In this simulation, $\mu(i_1,i_2) \equiv 1$, which means that a full coherent illumination is realized at the aperture of 100 μm $\times$ 100 μm placed 50 m downstream from an x-ray source, is predicted to be effective using the high-performance undulator of SPring-8 as an x-ray source. In a total reflection, the reflectivity at each point on the mirror surface is approximately constant. The phase change due to an evanescent wave field at each point on the mirror surface is already considered in the design of the mirror shape.

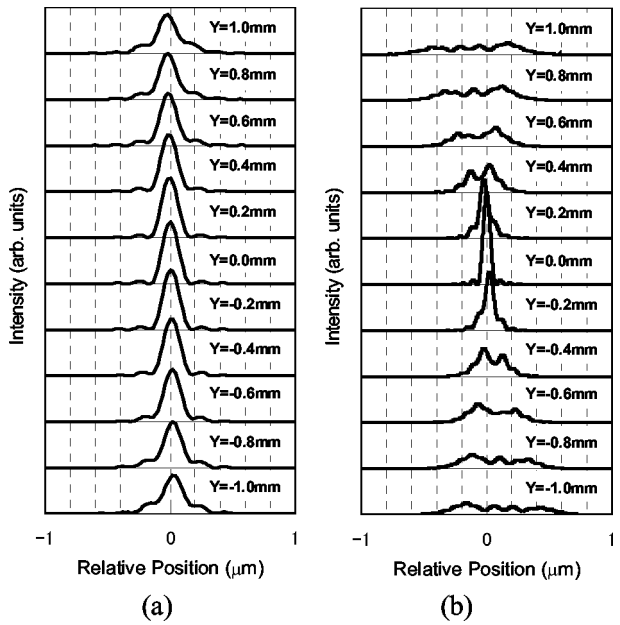

FIG. 7. Calculated beam waist structures in vertical and horizontal directions.

TABLE II. Summary of acceptable ranges of mirror alignments for realizing diffraction-limited focusing two-dimensionally at an x-ray energy of 15 keV.

	Glancing angle	Perpendicularity	In-plane rotation	Focal depth
Mirror A	±7 μmrad	±0.4 mrad	±65 mrad	±1.2 mm
Mirror B	±2 μrad		±40 mrad	±0.2 mm

B. Simulation results

Various glancing angle errors were given, and focused beam profiles were calculated wave optically. Figure 5 shows the beam profiles independently obtained in the vertical and horizontal directions. The relationship between beam size and glancing angle is shown in Fig. 6, where the beam size is FWHM. When the acceptable beam size broadening is within 20% of the ideal beam size, the angle errors should be smaller than ±7 μrad and ±2 μrad in the vertical and horizontal focusings, respectively.

In scanning x-ray microscopy, the displacement from the focal point along the beam axis should be smaller than the focal depth of the optical system. On the basis of the assumption that the mirror angles are perfectly adjusted, the focused beam profiles were investigated every 1 mm along the beam axis near the ideal focal point. As shown in Fig. 7, when the range of error tolerance in the focal length is defined as that in which the beam size broadening is smaller than 20% of the ideal beam size, the acceptable ranges in M_A and M_B are ±1.2 mm and ±0.2 mm, respectively. Such focal depths are sufficiently large for relatively thick samples to be observed. This advantage originates in the mirror design with the small glancing angle and the small numerical aparture (N.A.). The photon flux and the theoretical beam size are sacrificed. Because of such tradeoff relations, we should appropriately select mirror parameters for the application objectives.

V. COMPACT TWO-DIMENSIONAL FOCUSING UNIT

Accuracies to be realized in the mirror alignments are summarized in Table II. An x-ray focusing unit fulfilling the criteria was designed and actually constructed. The photograph of the unit is shown in Fig. 8(a). The glancing angle adjustment requires a higher accuracy than those of other alignment parameters; thus, the flexure hinges and the pulse-motor-based linear actuators are employed for the alignment

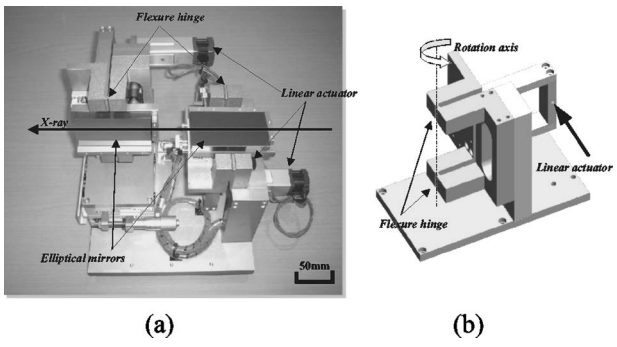

FIG. 8. Schematic views of the K-B focusing unit. (a) Photograph of the focusing unit. (b) Schematic drawing of the glancing angle adjuster.

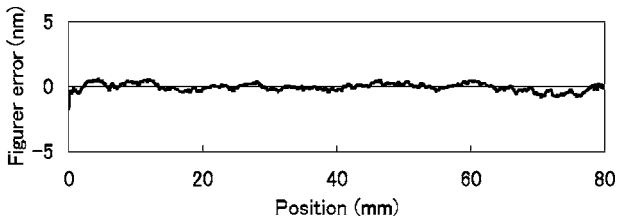

FIG. 9. Residual figure error profile of the M_A. The peak-to-valley and rms figure error are 26 and 0.2 nm.

of the glancing angle, as shown in Fig. 8(b). The mechanism adjusts the angles without any mechanical sliding and friction. The angular resolutions realized in the unit are 1 μrad in both M_A and M_B. The adjuster for the perpendicularity of the mirrors consists of two sets of linear actuators located under the vertical focusing mirror, and has an angular resolution of 0.2 mrad. In the in-plane rotation adjustment, micrometer heads are employed because the acceptable range is ±50 mrad. To minimize the elastic deformation of the mirrors by gravitational force, the mirrors are placed on mirror stages using three support balls arranged at Airy points. The elastic deformation was estimated using the finite element method, and a maximum deformation of less than 1 nm was confirmed.

VI. EXPERIMENTS ON FOCUSING PROPERTIES

The K-B focusing unit equipped with ultraprecise mirrors[10–14] fabricated by EEM,[15–17] P-CVM[18–20] and microstitching interferometry[11] was installed at BL29XUL, and tested in terms of two-dimensional focusing performance at an x-ray energy of 15 keV. The figure error of the M_A is shown in Fig. 9. Figure accuracy of M_B is in the same level of M_A. These accuracies are confirmed to be enough to realize diffraction-limited focusing.[6] The beam profile was measured by a wire scan method using a gold wire with a diameter of 200 μm. The perpendicularity of the two mirrors and the in-plane rotations were preadjusted to within acceptable errors. Figure 10 shows the tuning process of the glancing angle of M_A using a series of beam profiles at different glancing angle errors. The horizontal axis denotes the wire position, and the subscripts in the graph show the error values (in 10^{-6} rad) from the optimum glancing angle. The calculated beam profiles are shown in the same graph by solid lines, together with the measured profiles shown by dots. The measured results were in good agreement with the calculated ones.

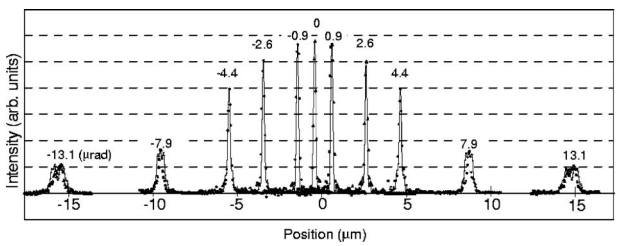

FIG. 10. Tuning process of the glancing angle of M_A using a series of beam profiles. The measured and wave-optically calculated profiles are shown by dots and solid lines, respectively.

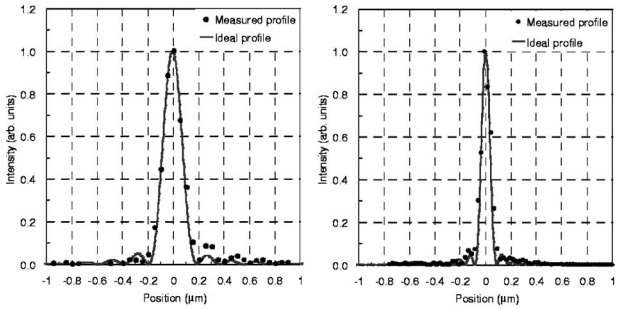

FIG. 11. Two-dimensional intensity profile experimentally obtained at the x-ray energy of 15 keV. (a) Vertical focusing (50 nm step); (b) horizontal focusing (25 nm step).

After adjusting the glancing angle, the two-dimensionally focused beam profile was measured and is shown in Fig. 11 together with the solid line of the beam profile calculated using the ideal mirror profile. A beam size of 180 nm(V) $\times$ 90 nm(H) in FWHM was achieved. The obtained results in the vertical and horizontal focusings are consistent with the calculated results and show that two-dimensional diffraction-limited focusing is realized. The measured profile is completely raw data without any compensation to take the transmission effect at the gold wire edge into account, because such influences only appear at the edge of focused profile with the width of smaller than 10 nm.

ACKNOWLEDGMENTS

This research was partially supported by a Grant-in-Aid for Scientific Research (S), 15106003, 2004 and the 21st Century COE Research, Center for Atomistic Fabricaton Technology, 2004 from the Ministry of Education, Culture, Sports, Science, and Technology of Japan.

[1] K. Yamauchi, K. Yamamura, H. Mimura, Y. Sano, A. Saito, A. Souvorov, M. Yabashi, K. Tamasaku, T. Ishikawa, and Y. Mori, J. Synchrotron Radiat. **9**, 313 (2002).
[2] K. Yamauchi, K. Yamamura, H. Mimura, Y. Sano, A. Saito, K. Endo, A. Souvorov, M. Yabashi, K. Tamasaku, T. Ishikawa, and Y. Mori, Jpn. J. Appl. Phys., Part 1 **42**, 7129 (2003).
[3] O. Hignette, P. Cloetens, W.-K. Lee, W. Ludwig, and G. Rostaing, J. Phys. IV **104**, 231 (2003).
[4] G. E. Ice, J.-S. Chung, J. Z. Tischler, A. Lunt, and L. Assoufid, Rev. Sci. Instrum. **71**, 2635 (2000).
[5] P. Naulleau, K. Goldberg, P. Batson, S. Jeong, and J. Underwood, Appl. Opt. **40**, 3703 (2001).
[6] K. Yamauchi, K. Yamamura, H. Mimura, Y. Sano, A. Saito, M. Kanaoka, K. Endo, A. Souvorov, M. Yabashi, K. Tamasaku, T. Ishikawa, and Y. Mori, Proc. SPIE **4782**, 271 (2002).
[7] P. Kirkpatrick and A. V. Baez, J. Opt. Soc. Am. **38**, 766 (1948).
[8] T. Ishikawa, K. Tamasaku, M. Yabashi, S. Goto, Y. Tanaka, H. Yamazaki, K. Takeshita, H. Kimura, H. Ohashi, T. Matsushita, and T. Ohata, Proc. SPIE **4154**, 1 (2001).
[9] M. Born and E. Wolf, *Principles of Optics*, 6th ed (Cambridge University Press, Cambridge, 1997).
[10] K. Yamamura, H. Mimura, K. Yamauchi, Y. Sano, A. Saito, T. Kinoshita, K. Endo, A. Souvorov, M. Yabashi, K. Tamasaku, T. Ishikawa, and Y. Mori, Proc. SPIE **4782**, 265 (2002).
[11] K. Yamauchi, K. Yamamura, H. Mimura, Y. Sano, A. Saito, K. Ueno, K. Endo, A. Souvorov, M. Yabashi, K. Tamasaku, T. Ishikawa, and Y. Mori, Rev. Sci. Instrum. **74**, 2894 (2003).
[12] Y. Mori, K. Yamauchi, K. Yamamura, H. Mimura, A. Saito, Y. Sano, K. Endo, A. Souvorov, M. Yabashi, K. Tamasaku, and T. Ishikawa, M. Shimura, and Y. Ishizaka, Proc. SPIE **5193**, 11 (2003).
[13] Y. Mori, K. Yamauchi, K. Yamamura, H. Mimura, Y. Sano, A. Saito, K. Ueno, K. Endo, A. Souvorov, M. Yabashi, K. Tamasaku, and T. Ishikawa, Proc. SPIE **5193**, 105 (2003).
[14] H. Mimura, K. Yamauchi, K. Yamamura, A. Kubota, S. Matsuyama, Y. Sano, K. Ueno, K. Endo, Y. Nishino, K. Tamasaku, M. Yabashi, T. Ishikawa, and Y. Mori, J. Synchrotron Radiat. **11**, 343 (2004).
[15] Y. Mori, K. Yamauchi, and K. Endo, Precis. Eng. **9**, 123 (1987).
[16] Y. Mori, K. Yamauchi, and K. Endo, Precis. Eng. **10**, 24 (1988).
[17] K. Yamauchi, H. Mimura, K. Inagaki, and Y. Mori, Rev. Sci. Instrum. **73**, 111 (2002).
[18] Y. Mori, K. Yamamura, and Y. Sano, Rev. Sci. Instrum. **71**, 4620 (2000).
[19] Y. Mori, K. Yamauchi, K. Yamamura, and Y. Sano, Rev. Sci. Instrum. **71**, 4627 (2000).
[20] K. Yamamura, K. Yamauchi, H. Mimura, Y. Sano, A. Saito, K. Endo, A. Souvorov, M. Yabashi, K. Tamasaku, T. Ishikawa, and Y. Mori, Rev. Sci. Instrum. **74**, 4549 (2003).